Flexible Polymer Rectifying Diode on Plastic Foils with MoO_3 Hole Injection

Miao Li[1], Nazmul Rafi[1], Paul R. Berger[1, 2], Donald Lupo[1], and Matti Mäntysalo[1]
[1]) Faculty of Information Technology and Communication Sciences, Tampere University, Finland
[2]) Electrical and Computer Engineering, The Ohio State University, Columbus, OH 43210, USA
miao.li@tuni.fi; matti.mantysalo@tuni.fi

***Abstract*— In this work, a flexible solution processed polymer diode with a structure of aluminum/indacenodithiophene-benzothiadiazole (C_{16}-IDT-BT)/molybdenum trioxide/gold was developed. A DC rectification ratio of 7×10^3 was achieved at 2 V with a forward current density of 2.6 mA/cm^2 and a reverse current density of 0.37 µA/cm^2. The UV-ozone treated MoO_3 layer acted as a hole injection layer for the C_{16}-IDT-BT layer to enhance the forward current density. The Au electrode with a higher work function compared to Ag was a superior anode for the polymer diode. The diode can be used as a blocking diode to allow the current to flow in the desired direction.**

Keywords*— organic, polymer diode, high DC rectification, solution processed, flexible electronics

I. Introduction

Organic semiconductors, especially conjugated polymers, are intrinsically solution processable at rather low temperatures, making them attractive materials for a range of flexible and printable devices and systems [1]–[7]. These inexpensive, flexible and printable organic devices can be realized for various emerging applications such as the increasing demand for Internet of Things (IoT), wireless sensors and other ubiquitous small and embedded electronics. One of the most urgent demands of IoT is innovative, sustainable energy supply solutions to power billions of small electronic devices. Harvesting energy, or energy scavenging, from ambient sources such as light, radio frequency radiation, motion or thermal energy has massive appeal [8] and liberates the systems to be sustainably autonomous. The harnessed energy can be stored in novel energy storage devices, such as low-cost, environmentally friendly supercapacitors to form an autonomous energy module powering embedded sensors [9], [10].

As the simplest active electronic components, printable diodes based on organic semiconductors are important building blocks for low-cost energy harvesting modules. Printed organic polymer diodes have been used extensively as rectifiers (and voltage multipliers) to convert RF energy to DC power [7], [11]–[14]. Previously, we have demonstrated printable RF energy harvesters with gravure printed organic poly(triarylamine) PTAA diodes operating at 13.56 MHz [7], [9]. However, organic diodes like their Si-based counterparts can be used in many other applications such as an active matrix driving circuit [15]. Our aim in this work is to develop a DC blocking diode as a power protection unit between the energy supply and the energy storage. The targeting voltage for the energy storage is around 2 V. Thus, the blocking diode should have a high current density at forward bias and a low reverse current density at reverse bias, in other words, a high DC rectification ratio at 2 V.

This work is sponsored by Business Finland through ECOtronics project (Grant Agreement Number 2660/31/2019. Parts of the research uses Academy of Finland Research Infrastructure "Printed Intelligence Infrastructure" (PII-FIRI, Grant Number 320019).

II. Experiments

Organic diodes were fabricated on both a SiO_2 coated wafer (31.500 Å ±5% Wet Thermal Oxide from Siegert Wafer) and a polyimide substrate (Kapton™ PV9100 from DuPont). The diode structure is shown in Fig. 1. A 45 nm thin layer of Al was E-beam evaporated through a shadow mask onto the substrate to form a cathode. A 5 mg/ml solution of indacenodithiophene-benzothiadiazole (C_{16}-IDT-BT from Flexink) in 1,2-dichlorobenzene (from Sigma-Aldrich) was spin coated at 1500 rpm for 1 minute. The solution was preheated on a hotplate at 85 ^{0}C for 30 minutes to enhance the solubility before spin-coating. In addition, the Al layer was exposed to UV-ozone for 10 minutes to improve the wetting of C_{16}-IDT-BT solution. The C_{16}-IDT-BT layer was then cured on a hotplate at 150 ^{0}C for 30 minutes. A 2 nm thin layer of MoO_3 was thermal evaporated through a shadow mask as a hole injection layer. The MoO_3 layer was treated with UV-ozone for 10 minutes to tune the work function. A 100 nm Au or Ag layer was successively thermally evaporated through the same shadow mask to form an anode. All the evaporation materials were purchased from Kurt J. Lesker. The UV-ozone treatment was done with a PSD-UV from Novascan. All fabrication steps, except the UV-ozone treatment, were carried out in a nitrogen-filled glovebox. The organic diodes were taken outside the glovebox after fabrication with no encapsulation and all characterization was done in ambient environment. In addition, for Kelvin probe force microscopy (KPFM) measurement, a 100 nm Au layer followed by a 2 nm MoO_3 layer were thermal evaporated consecutively on a SiO_2 coated wafer to assemble a MoO_3 thin film sample.

The diode area was defined by the cross section of all the layers, which was approximately 0.02 cm^2. The C_{16}-IDT-BT

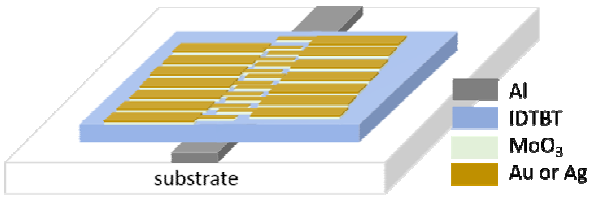

Fig. 1. Illustration of the diode structures.

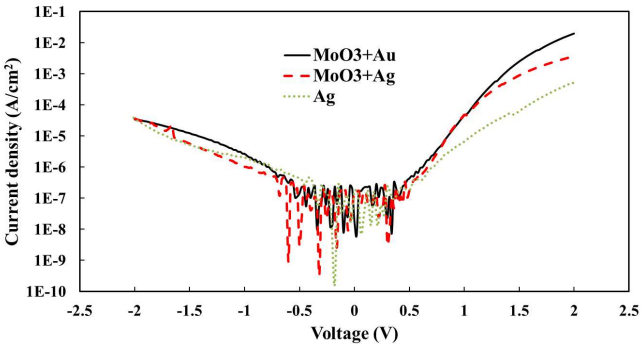

Fig. 2. J-V characteristics of C_{16}-IDT-BT diodes with different anode materials fabricated on SiO_2 wafer.

layer thickness was determined using a Bruker Dektak XT stylus profilometer. The layer thickness was around 200 nm on the SiO_2 wafer. The KPFM measurements were performed with a Bruker Dimension Icon in PeakForce KPFM mode. The current (current density)-voltage [I(J)-V] measurements of the organic diodes were carried out using a Keysight B1500A semiconductor analyzer connected to a probe station.

III. Results and Discussions

The intrinsic organic blocking diodes have a single semiconducting C_{16}-IDT-BT layer sandwiched between two metal electrodes, and modified versions with an additional buffer layer of MoO_3 at the anode reported here. Due to the undoped organic semiconductor properties, the C_{16}-IDT-BT diodes can be considered as a metal-insulator-metal (MIM) diode. For p-type organic semiconductor C_{16}-IDT-BT, the ohmic injection contact is achieved by selecting a metal with a higher work function than the highest occupied molecular orbital (HOMO) level of the polymer. This metal, as an anode, injects charge carriers, i.e., holes for p-type semiconductor, into the polymer under forward bias. On the other hand, a cathode electrode is realized by having a lower function metal compared to the HOMO level of the polymer. Their energy difference creates a barrier which blocks carriers to move under reverse bias. The reported HOMO level for C_{16}-IDT-BT is -5.4 eV [16]. This energy level is higher relative to most high work function metals such as Au (-5.1 eV), Pd (-5.12 eV), and Ni (-5.15 eV) [17], thus making it challenging to find a suitable anode electrode. Alternatively, transition metal oxide, such as molybdenum trioxide (MoO_3), has been widely reported as anode buffer layer to successfully enhance hole injection in organic diodes due to its reported high work function of approximately -6.6 eV [12], [18]–[20]. Thus, MoO_3 as the buffer layer was introduced in this report between the C_{16}-IDT-BT polymer and the anode metal. In addition, Al with a low work function around -4.2 eV [17] was fabricated as the cathode. The diodes were first fabricated on an SiO_2 coated wafer before exploring flexible polyimide substrates too.

As one of the more common anode materials for p-type organic semiconductors, silver was initially tested as an anode material [12], [21]. Additionally, gold with a high work function was also selected for these initial tests. Surprisingly the fabricated polymer diodes with the Ag electrode without any buffer layer showed a current density of 0.48 mA/cm^2 and a passable DC rectification ratio of 12 at 2 V as shown in Fig. 2. On the other hand, the fabricated diodes with the Au anode offered no rectification. It is

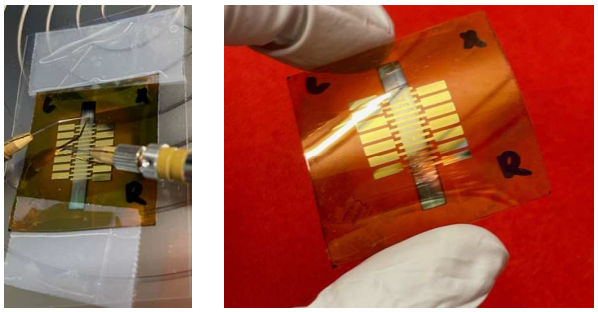

Fig.3. Photographs of the Al-(C_{16}-ID-TBT)-MoO_3-Au diodes on a flexible substrate.

interesting that Ag (4.7 eV) [17] with a lower work function than Au should theoretically act as an inferior hole injection anode, limiting the forward current. However, the J-V result showed passable forward current with Ag as the anode and no rectification with Au as the anode. We suspect the Ag electrode was oxidized during the fabrication process, modifying its work function, whereas the Au layer had poor contact properties, which could be due to a chemical reaction, diffusion, or poor adhesion of Au on the polymer.

Next, the MoO_3 as the buffer layer at the anode was tested. As shown in Fig. 2, diodes with MoO_3 as the buffer layer at the Ag anode yielded a significantly higher current density of 3.7 mA/cm^2 at 2 V. The forward current density increased approximately 8 times when adding the MoO_3 layer at the Ag anode. This clearly demonstrated that the MoO_3 layer can effectively enhance the hole injection into the polymer, thus increasing the forward current density of the diodes. Furthermore, as shown in Fig. 2, diodes with MoO_3-Au as the anode provided superior J-V characteristics, i.e., the highest forward current density while the reverse current density were similar to the Ag diodes. Compared to the diodes with MoO_3-Ag as the anode, the improved forward current of the diodes with the MoO_3-Au anode is likely due to the higher work function of the Au. In addition, the MoO_3 as the buffer layer also prevented a direct contact between C_{16}-IDT-BT and Au which we attributed to the lack of rectification of the diodes with only Au as the anode. To sum up, the initial tests on the SiO_2 coated wafers indicated that Al-(C_{16}-ID-TBT)-MoO_3-Au diodes offered the best performance. The forward and reverse current density were 19 mA/cm^2 at 2 V and 34 μA/cm^2 at -2 V, respectively. The resulting DC rectification ratio was 5.55×10^2 at 2 V.

Lastly, Al-(C_{16}-ID-TBT)-MoO_3-Au diodes were fabricated on flexible polyimide substrates, see Fig. 3. The fabrication steps are identical to the diodes on the SiO_2 coated wafers reported here. The J-V characteristics of the polymer diodes on polyimide substrates are shown in Fig. 4. The forward and reverse current density of Al-(C_{16}-ID-TBT)-MoO_3-Au diodes on polyimide were 2.8 mA/cm^2 at 2 V and 0.31 μA/cm^2 at -2 V, respectively. Compared to the wafer sample in Fig. 2, the forward current density of the polyimide sample decreased about 7 times while the reverse current dropped 100 times. This resulted an excellent DC rectification ratio of 9×10^3 at 2 V. The drastic reduction of current density from the polyimide sample is likely due to a slightly thicker C_{16}-IDT-BT layer caused by the different surface energy and roughness of the polyimide substrate compared to the SiO_2 coated wafer. Table I lists the major J-V parameters of diodes with different anode materials on both Si and polyimide substates.

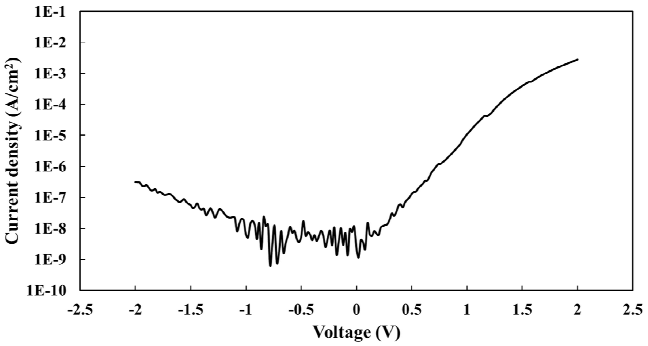

Fig. 4. J-V characteristics of Al-(C_{16}-ID-TBT)-MoO_3-Au diodes on a flexible substrate.

TABLE I. J-V PARAMETERS WITH DIFFERENT ANODE ELECTRODES

Anode	J @ 2 V (mA/cm2)	J @ -2 V (μA/cm2)	DC rectification ratio
Ag	0.48	38.6	12
MoO_3-Ag	3.7	36.7	100
MoO_3-Au	19	34.2	555
MoO_3-Au on PI	2.8	0.31	9000

As a hole injection, anode buffer layer, the work function of thermally evaporated MoO_3 layers was investigated more thoroughly. To ensure a sufficient conductivity of the film, a 100 nm Au layer was deposited under the 2 nm MoO_3 layer on the SiO_2 coated wafer. In addition, a conductive copper tape was placed on top of the MoO_3 layer and the sample holder to ground the sample. KPFM was used to measure the resulting work function, and KPFM showed the mean potential was 1.23 V for the as-deposited MoO_3 sample and 1.51 V for the UV-ozone treated MoO_3 sample, relative to the reference electrode. The resulting work functions were extracted for the as-deposited and UV-ozone treated MoO_3 samples, which were 6.03 eV and 6.31 eV, respectively. These values are within the reported work function range of MoO_3 [22], [23]. However, since the KPFM measured the contact potential, also called surface potential difference, between the tip and a sample (or between the ground and a sample) in the form of a capacitor. In this case, the MoO_3+Au layers acted as one of the plates of the capacitor. In other words, the measured potential represented all the induced charges at the surface which included the charges from the Au layer. Therefore, the calculated work function is not expected to be an accurate representation of the work function of the MoO_3 layer fabricated in this work. Nonetheless, the relative potential increase from 1.23 V to 1.51 V is entirely caused by the increased surface oxygen content of the MoO_3 layer from the UV-ozone treatment, which contributed to a 0.28 eV increase in work function of the treated MoO_3 layer. Indeed, the versatility of tuning work function of MoO_3 by inducing defects or changing the oxidation state of the metal cation is widely reported [18], [20]. In addition, the UV-ozone treatment removed a variety of contaminants from the MoO_3 layer surfaces to enable a consistent fabrication process. The RMS surface roughness as measured by AFM of the as-deposited and the UV-ozone treated MoO_3 samples is 1.11 nm and 0.892 nm, respectively. Similarly, KPMF results show the potential of UV-ozone treated Al increased by 0.6 V compared to the as-deposited Al layer which suggested the work function of Al changes from -4.2 eV to -4.8 eV. Therefore, the approximate energy

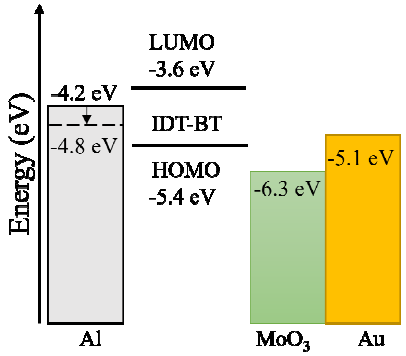

Fig. 5. Diagram of approximate energy levels of different layers.

levels for the various layers in the diodes are presented in Fig.5.

Besides the current density and the DC rectification ratio, another important parameter to evaluate for these diodes is the built-in voltage, which is sometimes referred as the turn-on voltage, or the threshold voltage. For undoped MIM type semiconductors, it is customarily defined as the work function difference of the two metal electrodes [24], [25]. However, in practice, several factors can affect the built-in voltage of the polymer diode such as the metal-organic interfaces formed by the printing process [26]–[28], and the trap states inside the organic layers [29]. Since the vacuum levels rarely align at the metal-organic interfaces, the relation of the work function and the energy alignment became more complicated [20], [30]. Therefore, in some studies the built-in voltage is determined as where the current starts to enter the space charge limited current (SCLC) region [24]. In other reports, the turn-on voltage is determined by the voltage where logJ has a sharp rise [31]. For the polymer diodes in this work, the diodes have not entered the SCLC region at 2 V, i.e., the current did not follow the Mott-Gurney equation [32]. In other words, the diodes were still in the diffusion and contact -limited current region [24] and the built-in voltage was larger than 2 V. Therefore, although the diodes offered high current density at low voltages (< 2 V) as well as excellent DC rectification ratio, the electrodes and the buffer layer should be able to be further optimized to lower the built-in voltage.

IV. CONCLUSION

This work demonstrates solution processed organic polymer C_{16}-ID-TBT diodes with different anode materials and a buffer layer. The UV-ozone treated MoO_3 layer as a hole injection buffer layer can significantly enhance the forward current density of the polymer diode. As an anode, Au with a higher work function yielded a larger forward current density compared to Ag. The polymer diode with a structure of Al-(C_{16}-ID-TBT)-MoO_3-Au was fabricated on a flexible polyimide substrate. At ±2V the forward current density was 2.6 mA/cm^2 whereas the reverse current was 0.37 μA/cm^2. The resulting DC rectification was 7×10^3. All the measurements were performed in air. With further optimization of the MoO_3 layer, the IV characteristics of the polymer diodes can be improved.

ACKNOWLEDGMENT

The authors would like to thank Turkka Salminen at Tampere Microscopy Center (TMC) for their support in KPFM measurements.

REFERENCES

[1] G. Grau and V. Subramanian, "Fully High-Speed Gravure Printed, Low-Variability, High-Performance Organic Polymer Transistors with Sub-5 V Operation," *Adv. Electron. Mater.*, vol. 2, no. 4, pp. 1–8, 2016, doi: 10.1002/aelm.201500328.

[2] S. Chung, K. Cho, and T. Lee, "Recent Progress in Inkjet-Printed Thin-Film Transistors," *Adv. Sci.*, vol. 6, no. 6, 2019, doi: 10.1002/advs.201801445.

[3] A. Kim, H. Lee, C. Ryu, S. M. Cho, and H. Chae, "Nanoscale thickness and roughness control of gravure printed MEH-PPV layer by solvent printing for organic light emitting diode," *J. Nanosci. Nanotechnol.*, vol. 10, no. 5, pp. 3326–3330, 2010, doi: 10.1166/jnn.2010.2283.

[4] R. Valmiro, H. Kitaguti, and S. E. Barbin, "A silk-screen printed RFID tag antenna," *2015 Asia-Pacific Microw. Conf. Proceedings, APMC*, vol. 3, pp. 9–11, 2015, doi: 10.1109/APMC.2015.7413586.

[5] C. Martínez-Domingo, S. Conti, L. Terés, H. L. Gomes, and E. Ramon, "Novel flexible inkjet-printed Metal-Insulator-Semiconductor organic diode employing silver electrodes," *Org. Electron.*, vol. 62, no. August, pp. 335–341, 2018, doi: 10.1016/j.orgel.2018.08.011.

[6] M. M. Laurila *et al.*, "A fully printed ultra-thin charge amplifier for on-skin biosignal measurements," *IEEE J. Electron Devices Soc.*, vol. 7, no. February, pp. 566–574, 2019, doi: 10.1109/JEDS.2019.2915028.

[7] M. Li *et al.*, "All Printed Large Area E-field Antenna Utilizing Printed Organic Rectifying Diodes for RF Energy Harvesting," *Proc. IEEE Conf. Nanotechnol.*, vol. 2018-July, 2019, doi: 10.1109/NANO.2018.8626318.

[8] H. Jayakumar, K. Lee, W. S. Lee, A. Raha, Y. Kim, and V. Raghunathan, "Powering the Internet of Things," *Proc. Int. Symp. Low Power Electron. Des.*, vol. 2015-Octob, pp. 375–380, 2015, doi: 10.1145/2627369.2631644.

[9] S. Lehtimäki *et al.*, "Performance of printable supercapacitors in an RF energy harvesting circuit," *Int. J. Electr. Power Energy Syst.*, vol. 58, pp. 42–46, 2014, doi: 10.1016/j.ijepes.2014.01.004.

[10] M. Arvani *et al.*, "Flexible energy supply for distributed electronics powered by organic solar cell and printed supercapacitor," *Proc. IEEE Conf. Nanotechnol.*, vol. 2020-July, pp. 257–262, 2020, doi: 10.1109/NANO47656.2020.9183493.

[11] C. Y. Lin, C. H. Chou, T. S. Hu, and J. Hou, "Flexible wireless power-transmission system fabricated by 13.56 MHz polymer rectifier," 2008, doi: 10.1109/FEDC.2008.4483870.

[12] S. G. Higgins, T. Agostinelli, S. Markham, R. Whiteman, and H. Sirringhaus, "Organic Diode Rectifiers Based on a High-Performance Conjugated Polymer for a Near-Field Energy-Harvesting Circuit.," *Adv. Mater.*, vol. 29, no. 46, Dec. 2017, doi: 10.1002/adma.201703782.

[13] C. Y. Lin *et al.*, "High-frequency polymer diode rectifiers for flexible wireless power-transmission sheets," *Org. Electron.*, vol. 12, no. 11, pp. 1777–1782, 2011, doi: 10.1016/j.orgel.2011.07.006.

[14] F. A. Viola *et al.*, "A 13.56 MHz Rectifier Based on Fully Inkjet Printed Organic Diodes," *Adv. Mater.*, vol. 32, no. 33, pp. 1–7, 2020, doi: 10.1002/adma.202002329.

[15] K. E. Lilja, T. G. Bäcklund, D. Lupo, J. Virtanen, E. Hämäläinen, and T. Joutsenoja, "Printed organic diode backplane for matrix addressing an electrophoretic display," *Thin Solid Films*, vol. 518, no. 15, pp. 4385–4389, 2010, doi: 10.1016/j.tsf.2010.02.008.

[16] W. Zhang *et al.*, "Indacenodithiophene semiconducting polymers for high-performance, air-stable transistors," *J. Am. Chem. Soc.*, vol. 132, no. 33, pp. 11437–11439, 2010, doi: 10.1021/ja1049324.

[17] J. Hölzl, F. K. Schulte, and H. Wagner, Eds., *Solid Surface Physics*, vol. 85. Berlin, Heidelberg: Springer Berlin Heidelberg, 1979.

[18] K. Kanai *et al.*, "Electronic structure of anode interface with molybdenum oxide buffer layer," *Org. Electron.*, vol. 11, no. 2, pp. 188–194, 2010, doi: 10.1016/j.orgel.2009.10.013.

[19] Z. Lü *et al.*, "Ohmic contact and space-charge-limited current in molybdenum oxide modified devices," *Phys. E Low-Dimensional Syst. Nanostructures*, vol. 41, no. 10, pp. 1806–1809, 2009, doi: 10.1016/j.physe.2009.07.003.

[20] M. T. Greiner, M. G. Helander, W. M. Tang, Z. Bin Wang, J. Qiu, and Z. H. Lu, "Universal energy-level alignment of molecules on metal oxides," *Nat. Mater.*, vol. 11, no. 1, pp. 76–81, 2012, doi: 10.1038/nmat3159.

[21] K. Lilja, "Performance, Interfacial Properties and Applications of Printed Organic Diodes," Tampere University of Technology, 2011.

[22] Y. Guo and J. Robertson, "Origin of the high work function and high conductivity of MoO3," *Appl. Phys. Lett.*, vol. 105, no. 22, pp. 1–5, 2014, doi: 10.1063/1.4903538.

[23] M. T. Greiner, L. Chai, M. G. Helander, W.-M. Tang, and Z.-H. Lu, "Metal/Metal-Oxide Interfaces: How Metal Contacts Affect the Work Function and Band Structure of MoO 3," *Adv. Funct. Mater.*, vol. 23, no. 2, pp. 215–226, Jan. 2013, doi: 10.1002/adfm.201200993.

[24] P. De Bruyn, A. H. P. Van Rest, G. A. H. Wetzelaer, D. M. De Leeuw, and P. W. M. Blom, "Diffusion-limited current in organic metal-insulator-metal diodes," *Phys. Rev. Lett.*, vol. 111, no. 18, 2013, doi: 10.1103/PhysRevLett.111.186801.

[25] W. Brütting, S. Berleb, and A. G. Mückl, "Device physics of organic light-emitting diodes based on molecular materials," *Org. Electron.*, vol. 2, no. 1, pp. 1–36, 2001, doi: 10.1016/S1566-1199(01)00009-X.

[26] Y. Shen, A. R. Hosseini, M. H. Wong, and G. G. Malliaras, "How to make ohmic contacts to organic semiconductors," *ChemPhysChem*, vol. 5, no. 1, pp. 16–25, 2004, doi: 10.1002/cphc.200300942.

[27] S. Braun, W. R. Salaneck, and M. Fahlman, "Energy-level alignment at organic/metal and organic/organic interfaces," *Adv. Mater.*, vol. 21, no. 14–15, pp. 1450–1472, 2009, doi: 10.1002/adma.200802893.

[28] S. Duhm, "5 - Interface energetics in organic electronic devices," in *Organic Flexible Electronics*, P. Cosseddu and M. Caironi, Eds. Woodhead Publishing, 2021, pp. 143–164.

[29] W. J. Lee *et al.*, "Improving turn on voltage and driving voltage of organic electroluminescent devices with nitrogen doped electron transporter," *Solid. State. Electron.*, vol. 47, no. 5, pp. 927–929, 2003, doi: 10.1016/S0038-1101(02)00393-3.

[30] P. S. Davids, I. H. Campbell, and D. L. Smith, "Device model for single carrier organic diodes," *J. Appl. Phys.*, vol. 82, no. 12, pp. 6319–6325, 1997, doi: 10.1063/1.366522.

[31] I. W. Wu, Y. H. Chen, P. S. Wang, C. G. Wang, S. H. Hsu, and C. I. Wu, "Correlation of energy band alignment and turn-on voltage in organic light emitting diodes," *Appl. Phys. Lett.*, vol. 96, no. 1, pp. 1–4, 2010, doi: 10.1063/1.3282682.

[32] A. Rose, "Space-charge-limited currents in solids," *Phys. Rev.*, vol. 97, no. 6, pp. 1538–1544, 1955, doi: 10.1103/PhysRev.97.1538.